

Supporting Information

Petit et al. 10.1073/pnas.1207634109

SI Text

Near-Critical Micellar Phases of Microemulsion. We used a near-critical phase-separated micellar solution of a microemulsion because, as illustrated below, supramolecular liquids have many advantages when investigating hydrodynamics near a critical point. The chosen microemulsion is a four-component liquid mixture composed of water, oil (toluene), surfactant (SDS), and cosurfactant (1-butanol-1). At low concentrations in water and surfactant, the quaternary mixture can in fact be considered as binary because it organizes at thermodynamic equilibrium as a suspension of surfactant-coated water nanodroplets, the micelles, dispersed in a continuum mainly composed of toluene. In the considered part of the phase diagram, a line of low critical points exists, the coexistence curves being inverted compared with the usual case (1). For the chosen composition [toluene: 70% (wt), water: 9% (wt), SDS: 4% (wt), and butanol: 17% (wt)], the micelle size, given by the amplitude factor of the correlation length of density fluctuations, is $\xi_0^+ = 40 \text{ \AA}$ (2). This value is sufficiently small for the mixture to be transparent in the visible range and large enough, typically $10\times$ that of classical fluids, to facilitate observation of critical opalescence. This micellar phase of microemulsion is isotropic and belongs to the universality class ($d = 3, n = 1$) of the Ising model (3), as most of classical liquid mixtures. For the chosen composition, the critical temperature is $T_C \approx 35^\circ\text{C}$. Above T_C , the mixture separates in two micellar phases of different micelle concentrations $\Phi_{i=1,2}$, as indicated in the schematic phase diagram shown in Fig. S1A. Many fluid properties present scaling-law behavior in $(T - T_C)$ near the critical point. Of interest for the present investigation are the following:

- i) The bulk correlation length of density fluctuations in the two-phase region: $\xi^- = \xi_0^- \left(\frac{T-T_C}{T_C}\right)^{-\nu}$ with $\nu = 0.63$ and $\xi_0^- = \xi_0^+ / 1.9 = (21 \pm 1) \text{ \AA}$.
- ii) The coexistence curve, assumed to be symmetric close to the critical point: $\Phi_{i=1,2} = \Phi_C + (-1)^i \frac{\Delta\Phi_0}{2} \left(\frac{T-T_C}{T_C}\right)^\beta$ with $\beta = 0.325$, $\Phi_C = 0.11$, and $\Delta\Phi_0 = 0.42$.
- iii) The density of the coexisting phases: $\rho_{i=1,2} = \rho_{mic} + \rho_{cont}(1 - \Phi_i)$, where $\rho_{mic} = 1,045 \text{ kg/m}^3$ and $\rho_{cont} = 850 \text{ kg/m}^3$ are the densities of the micelles and the surrounding oil continuum, respectively.
- iv) The interfacial tension between the coexisting phases: $\gamma = \gamma_0 \left(\frac{T-T_C}{T_C}\right)^{2\nu}$ with $\gamma_0 = 0.108 \times k_B T_C / (\xi_0^-)^2 = 10^{-4} \text{ N.m}^{-1}$ (ref. 4).
- v) The shear viscosity of the coexisting phases: $\eta_{i=1,2} = [1.460 - 0.014(T - 273.15)](1 + 2.5\Phi_i)10^{-3} \text{ Pa.s}$ (ref. 5).
- vi) The optical absorption at the used wavelength: $\alpha_{abs}(\lambda_0 = 532 \text{ nm}) \approx 0.03 \text{ m}^{-1}$, which prevents the mixture from laser heating at the used beam powers.

Generating Liquid Columns. The experimental procedure to produce stable liquid columns is presented in Fig. S1B. A laser beam

is focused on the meniscus of the phase-separated mixture (contained in a 1- or 2-mm-thick sealed Hellma cell) using a $10\times$ Olympus microscope objective (N.A. = 0.25). The beam power and the beam waist ω_0 can be changed using various optical components. Because the interfacial tension of near-critical interfaces is extremely weak, meniscus deformations are induced by the radiation pressure of the continuous laser beam, here a frequency-doubled $Nd^{3+} - YAG$ (wavelength in vacuum $\lambda_0 = 532 \text{ nm}$) in the TEM_{00} mode. The interface bending direction does not depend on beam propagation because photons gain momentum when crossing the interface from a low to a large refractive index medium. Consequently, momentum conservation always leads to a meniscus bending toward the fluid of smallest index of refraction, i.e., here from Φ_2 to Φ_1 , because (i) Φ_2 is the liquid phase of lowest micellar concentration and (ii) the index of refraction of toluene is larger than that of water. Nonetheless, the generation of stable liquid columns (Fig. S1 C and D) requires a beam incidence from the fluid of largest index of refraction (6), i.e., the liquid phase Φ_2 . The beam should then propagate downward as indicated by the arrow in Fig. S1C. Above a beam power threshold, the bended meniscus becomes unstable, forms a jet, and produces a stable liquid column when the jet tip reaches the bottom face of the cell containing the sample. Comparison between Fig. S1 C and D shows that the column radius can be tuned by varying the beam power. Observations are performed from the side using a focused white-light source for illuminating the sample and a $50\times$ Olympus microscope objective (N.A. = 0.45) for imaging using a video camera and recording the destabilization of the liquid columns when the laser is turned off. A spectral filter is also placed between the microscope and the camera to eliminate the laser light scattered by the micellar phases near the critical point.

Contactless Measurement of the Interfacial Tension. The measurement of ultralow interfacial tensions is very difficult by usual contact techniques. We thus used the radiation pressure of the laser beam at low beam power to deform the meniscus separating the two coexisting phases and deduce γ at a given $(T - T_C)$ from the stationary deformation height $h(r = 0)$ on beam axis (7). In the weak deformation regime ($\partial h / \partial r \ll 1$), this height is given

by $h(r = 0) = \left(\frac{-2P}{cg\alpha\omega_0^2}\right) \left(\frac{\partial n}{\partial \rho}\right)_T \frac{\omega_0^2}{8l_c^2} \exp\left(\frac{\omega_0^2}{8l_c^2}\right) E_1\left(\frac{\omega_0^2}{8l_c^2}\right)$, where $(\partial n / \partial \rho)_T$ is

the refractive index variation with density, $l_c = \sqrt{\frac{\gamma}{(\rho_1 - \rho_2)g}}$ is the capillary length, and $E_1(x)$ is the exponential integral function (6). For example, we find $h(r = 0) = -5.5 \pm 0.3 \mu\text{m}$ for an experiment performed at $(T - T_C) = 0.3 \text{ K}$, $\omega_0 = 7.48 \mu\text{m}$, and $P = 33 \text{ mW}$; and $h(r = 0) = -8.0 \pm 0.3 \mu\text{m}$ at $(T - T_C) = 0.4 \text{ K}$, $\omega_0 = 7.48 \mu\text{m}$, and $P = 66 \text{ mW}$; the uncertainties on $h(r = 0)$ results from the use of a $20\times$ objective, instead of $50\times$, for imaging the entire interface deformation. We respectively deduce $\gamma \approx 1.8 \cdot 10^{-8} \text{ N/m}$ and $\gamma \approx 2.6 \cdot 10^{-8} \text{ N/m}$. Taking into account the uncertainty on $h(r = 0)$, the estimation of $(\partial n / \partial \rho)_T$ from the Clausius-Mossotti relation, and the relative error $\leq 10\%$ on $(T - T_C)$ at $(T - T_C) = 0.3 - 0.4 \text{ K}$, we find a deviation $\leq 20\%$ on γ compared with the value calculated from the universal ratio \mathfrak{R}^- .

1. Meunier J, Cazabat AM, Langevin D, Pouchelon A (1982) Critical behaviour in microemulsions. *J Phys Lett* 43(3):89-95.
2. Freysz E, Laffon E, Delville JP, Ducasse A (1994) Phase conjugation in critical microemulsions. *Phys Rev E Stat Phys Plasmas Fluids Relat Interdiscip Topics* 49(3):2141-2149.

3. Jean-Jean B, Freysz E, Ducasse A, Pouligny B (1988) Thermodiffusive and electrostrictive optical nonlinearities in critical microemulsions. *Europhys Lett* 7(3):219-224.
4. Moldover MR (1985) Interfacial tension of fluids near critical points and two-scale-factor universality. *Phys Rev A* 31(2):1022-1033.

5. Wunenburger R, et al. (2011) Fluid flows driven by light scattering. *J Fluid Mech* 666: 273–307.
6. Wunenburger R, Casner A, Delville JP (2006) Light-induced deformation and instability of a liquid interface. I. Statics. *Phys Rev E Stat Nonlin Soft Matter Phys*, 73(3):036314.

7. Mitani S, Sakai K (2002) Measurement of ultralow interfacial tension with a laser interface manipulation technique. *Phys Rev E*, 66(3):031604.

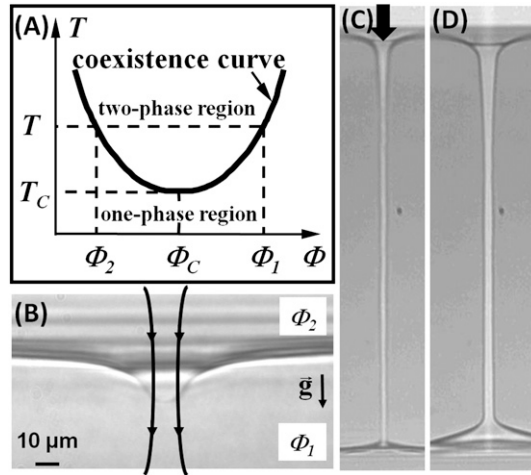


Fig. S1. (A) Schematic phase diagram of the micellar phase of microemulsion used. T is temperature and Φ is the volume fraction of micelles; T_C is the critical temperature and Φ_1 and Φ_2 are, respectively, the volume fractions of the micelle-rich and -poor phases in coexistence. (B) Experimental configuration for a temperature $T > T_C$. The optical bending of the meniscus of the phase-separated liquid mixture is driven by the optical radiation pressure of the laser beam, represented by the arrows. (C) Thinnest stable large-aspect-ratio liquid column obtained at $(T - T_C) = 4$ K for a beam power $P = 410$ mW and a waist $\omega_0 = 3.5$ μm . (D) Tuning of the liquid column diameter with further increase of the beam power to $P = 1,134$ mW. The liquid column length is 334 μm .